

Hypovalent Radicals. 4.¹ Gas-Phase Studies of the Ion-Molecule Reactions of Cyclopentadienylidene Anion Radical in a Flowing Afterglow

Richard N. McDonald,* A. Kasem Chowdhury, and D. W. Setser

Contribution from the Department of Chemistry, Kansas State University, Manhattan, Kansas 66506. Received December 26, 1979

Abstract: The carbene anion radical, cyclopentadienylidene⁻ ($c\text{-C}_5\text{H}_4^{\cdot-}$, **1**), was generated by dissociative electron attachment with diazocyclopentadiene (**2**) in a flowing afterglow apparatus. The ion-molecule reaction of **1** with **2** produced $c\text{-C}_5\text{H}_4\text{N}=\text{N}-c\text{-C}_5\text{H}_4^{\cdot-}$, $c\text{-C}_5\text{H}_4=c\text{-C}_5\text{H}_4^{\cdot-}$, and $c\text{-C}_5\text{H}_5^{\cdot-}$ by coupling at N_β and C_1 of **2** and H \cdot abstraction from **2**, respectively. The $\text{PA}(\mathbf{1}) = 377 \pm 2 \text{ kcal mol}^{-1}$ was determined from bracketing reactions of $\text{ROH} + \mathbf{1} \rightarrow \text{RO}^- + c\text{-C}_5\text{H}_5^{\cdot-}$, which gives $\Delta H_f^\circ(\mathbf{1}) = 70.7 \pm 3.2 \text{ kcal mol}^{-1}$. Although the H \cdot abstraction process by **1** was observed in most of its ion-molecule reactions, **1** failed to react with CH_4 , C_2H_4 , and $c\text{-C}_3\text{C}_6$ probably because of an activation barrier of $\geq 3 \text{ kcal mol}^{-1}$ in these cases. With dipolar CH_3OH and **1**, the only observed reaction was H \cdot abstraction from the O-H bond (shown with CH_3OD). This lower limit of the H \cdot affinity of **1** gives $\Delta H_f^\circ(\mathbf{1}) \geq 67.7 \pm 3 \text{ kcal mol}^{-1}$, in excellent agreement with the value derived from protonation studies. The reactions of **1** with CH_3X (Cl, Br) occur by H \cdot abstraction and halide ion ($\text{S}_{\text{N}}2$) displacement. Anion radical **1** adds to activated olefins $\text{H}_2\text{C}=\text{CHX}$ (CN, CO_2CH_3 , Cl) by a nucleophilic Michael addition mechanism. The EA of the carbene $c\text{-C}_5\text{H}_4$ was bracketed by charge-transfer reactions between **1** and C_6F_6 and NO_2 . All of these and certain other results are consistent with the $\sigma^1\pi^2$ electronic configuration as the ground state of **1**. The reactions of **1** with alcohols are postulated to proceed via a hydrogen-bonded complex.

Introduction

In 1977, we published our initial results of the electrochemical generation of diphenylcarbene anion radical and the characterization of certain of its reactions in solution.² Related electrochemical^{2,3} and chemical¹ studies with various carbene anion radical precursors have yielded valuable information on the reactivities of such *hypovalent radicals*⁴ in solution. However, the roles of solvation, ion pairing, and other condensed-phase factors on the chemistry of the reactive intermediates can only be crudely approximated at the present time. Furthermore, both electrochemical and chemical preparation methods of carbene anion radicals (reduction of diazo compounds) suffer in that it is not possible to have a variety of neutral reactants present with which to examine potentially important ion-molecule processes of these hypovalent anion radicals.

At the outset of our investigations of the chemistry of hypovalent radicals, parallel gas-phase and condensed-phase studies were planned. Of the powerful gas-phase techniques, e.g., ion cyclotron resonance spectrometry,⁵ high-pressure mass spectrometry,⁶ and the flowing afterglow,⁷ usually associated with ion-molecule reactions, the flowing afterglow was chosen for the following reasons: (a) the ionic and neutral reactant species have thermal energy distributions (Maxwell-Boltzmann), (b) a great variety of both ionic and neutral reactants have been studied,⁸ (c) ion sources are readily varied from "cool" (thermal e^- attachment \rightarrow negative ions) to "hot" methods (microwave discharge and electron impact), (d) accurate kinetic measurements can be done since time is given by (length of the reaction tube)/(average transport velocity of the ions), and (e) one of us (D.W.S.) had considerable experience

with the flowing afterglow technique.

This paper reports the gas-phase generation of cyclopentadienylidene anion radical (**1**) in a flowing afterglow (FA) apparatus. The ion-molecule reactions of **1** with various neutral reactants demonstrate the multifaceted reactivity of this carbene anion radical as (i) a free radical, (ii) a nucleophile, (iii) a base toward proton donors, and (iv) an electron-transfer agent.

The generation of **1** and study of its reactions in the gas-phase are of immediate interest to the condensed-phase work since **1** is the core structure of fluorenylidene anion radical ($\text{Fl}^{\cdot-}$), which is a relatively stable carbene anion radical in solution.^{1,3} Since certain reactions of $\text{Fl}^{\cdot-}$ in the condensed phase are well characterized, related processes for **1** in the gas phase should be expected. These would substantiate the anticipated structure of **1** and the reaction products predicted from that structure.

The structure of **1**, as well as the triplet and singlet carbenes, cyclopentadienylidene, were examined using MINDO/3⁹ and GEOMIN-INDO¹⁰ (both without CI) calculations. Both methods give the ground-state electronic configuration of **1** as a σ radical π anion ($\sigma^1\pi^2$). This $\sigma^1\pi^2$ configuration is consistent with the ESR spectrum obtained by photolysis (UV filter) of sodium and diazocyclopentadiene (**2**) in an argon matrix at 4 K.¹¹

Experimental Section

The FA apparatus used in the experiments reported in this paper was similar in design to that developed by Ferguson, Fehsenfeld, and Schmeltekopf and co-workers at the National Oceanic and Atmospheric Administration (NOAA) laboratories in Boulder, Colo.^{7,12}

A large flow of helium buffer gas (flow and pressure monitored with a calibrated triflat flowmeter and Celsco 0-900 Torr pressure transducer, respectively) is purified by passage through two traps filled with Davison 4A molecular sieves cooled with liquid nitrogen. After warming to room temperature in a glass coil, the buffer gas enters the upstream end of a $120 \times 7.15 \text{ cm i.d.}$ stainless steel reaction tube and is dispersed

(1) For part 3 in this series, see: McDonald, R. N.; Lin, K.-W. *J. Am. Chem. Soc.* **1978**, *100*, 8028.

(2) McDonald, R. N.; January, J. R.; Borhani, K. J.; Hawley, M. D. *J. Am. Chem. Soc.* **1977**, *99*, 1268.

(3) McDonald, R. N.; Borhani, K. J.; Hawley, M. D. *J. Am. Chem. Soc.* **1978**, *100*, 995.

(4) We define a "hypovalent radical" as a neutral or charged radical species containing less than the number of attached substituents found in the uncharged, free radical system normally associated with the central atom in the radical.

(5) Beauchamp, J. L. *Annu. Rev. Phys. Chem.* **1971**, *22*, 527.

(6) Kebarle, P. *Annu. Rev. Phys. Chem.* **1977**, *28*, 445.

(7) Ferguson, E. E.; Fehsenfeld, F. C.; Schmeltekopf, A. L. *Adv. At. Mol. Phys.* **1969**, *5*.

(8) Albritton, D. L. *At. Data Nucl. Data Tables* **1978**, *22*, 1-101.

(9) (a) We wish to thank Professor S. D. Worley, Auburn University, for making this program written for an IBM-370 computer available to us, and Professor Keith Purcell for his efforts to get it running on our machine. (b) Bingham, R. C.; Dewar, M. J. S.; Lo, D. H. *J. Am. Chem. Soc.* **1978**, *97*, 1285, 1294, 1302, 1307.

(10) Purcell, K. F. Quantum Chemistry Program Exchange, University of Indiana, Bloomington, Ind., No. 312.

(11) Kasai, P. H.; McLeod, D.; McDonald, R. N., unpublished results.

(12) Drs. Dan Albritton (NOAA) and Veronica Bierbaum (University of Colorado) were helpful with general and specific suggestions during construction and testing of the flowing afterglow.

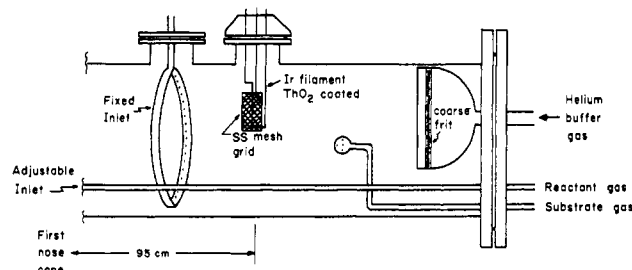


Figure 1. Ion preparation region of flowing afterglow apparatus.

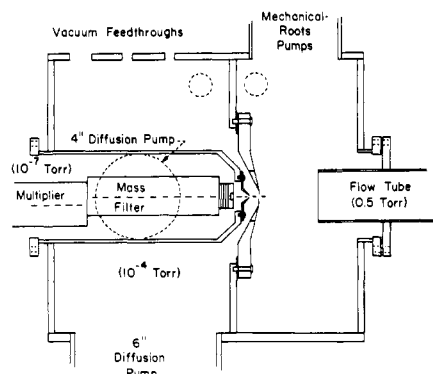


Figure 2. Differentially pumped analysis section of flowing afterglow apparatus.

through a coarse glass fritted disk funnel (see Figure 1). A fast helium flow of ca. 80 m s^{-1} is established in the tube by means of a Stokes Roots blower-mechanical pump system (Model 1722-S). With a helium flow of $206 \text{ atm cm}^3 \text{ s}^{-1}$ and partially throttled pumping speed, the helium pressure in the flow tube was typically ca. 0.5 Torr.

Ion production is generally accomplished by adding a substrate gas upstream of the electron gun, which consists of a heated thorium oxide coated iridium filament (H-P power supply; $\sim 3 \text{ V}$, 6 A) with a superimposed variable -30 to -100 voltage (Keithley power supply) relative to a grounded stainless steel mesh accelerating grid. Negative ions can be generated directly by electron attachment or indirectly by ion-molecule reactions. Alternatively, the substrate gas can be introduced through the fixed inlet located 6 cm downstream from the electron gun. In some instances, e.g., with SF_6 , less fragmentation of the desired ion (SF_6^-) was observed with this addition mode. The fixed inlet was a loop of 2 mm i.d. Teflon tubing with holes drilled every 5 mm on the inside of the loop.

The first 30 cm of the reaction tube downstream from the ionizer is a region for ion production and thermalization, and allows for full development of a laminar velocity profile and attenuation of higher diffusion modes. The remaining 65 cm of the flow tube before the first nose cone constitutes the reaction region of the ions with added neutral reactant gases. These reactant gases can be added through fixed inlets or through a movable stainless steel inlet (same description as above fixed inlet, but the loop is stainless steel) fitted through the outer flange with an O-ring slide-seal.

The reaction mixture exits the flow tube into the differentially pumped analysis chamber where most of the flow is exhausted by the Stokes blower-pump system (Figure 2). A fraction of the gas mixture is sampled through a 1.4-mm orifice in a molybdenum nose cone into the second compartment of the chamber (ca. 10^{-4} Torr) pumped by a Varian 6-in. oil diffusion pump backed by a mechanical pump. This portion of the reaction mixture is further sampled through a 1-mm orifice in a second molybdenum nose cone into the mass spectrometer-electron multiplier compartment normally operating at 2×10^{-7} Torr pumped by a Varian 4-in. oil diffusion pump backed by a mechanical pump. The second and third compartments are separated from the oil diffusion pumps by Varian cryotrap cooled by liquid nitrogen. The molybdenum nose cones are electrically isolated by Teflon gaskets from the main chamber housing (stainless steel). Electrical feedthroughs allow each molybdenum nose cone to be biased with a variable potential of 0 to $\pm 15 \text{ V}$ relative to ground. In the present work, the first nose cone was biased nominally at -0.5 V , and the second nose cone biased at $+15 \text{ V}$.

The Extranuclear quadrupole mass spectrometer has its own ionizer-lens system in front of the mass filter. It can be operated as a conventional low-pressure mass spectrometer (an external sample inlet directly into this compartment), or as an ion monitoring system for the flowing afterglow with the ability to apply separate bias potentials to each

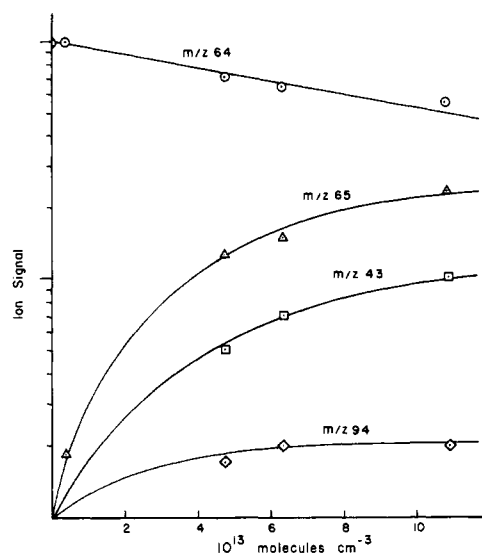


Figure 3. Semilogarithmic plot of decay of the parent ion and formation of products from channels 7a-c for the reaction of 1 + ethylene oxide. Ion signals are in arbitrary units. Formation of ion 15 (m/z 108) was omitted for clarity.

component of the ionizer-lens system. While various advantages are accrued in this arrangement, the presence of an additional sampling nose cone and the lens system of the mass spectrometer may significantly increase problems of mass discrimination and make measurements of ion-molecule product ion ratios, which are important in determining branching ratios, more difficult. The nominal mass range of the quadrupole is 0–500 amu. Electron multiplication employs a Bendix Channeltron (no. 4700) multiplier. The spectrometer is switchable to positive or negative ion detection.

In the present experiments, the neutral reactant gases were added through a fixed inlet 61 cm upstream from the first nose cone. The diazo compound 2 was added upstream of the electron gun and came in contact only with glass and Teflon O-ring valves (Kontes) before introduction into the flow tube. Flows of both the neutral reactant and the diazo compound were measured by determining the increase of pressure (calibrated pressure transducers) in a calibrated volume as a function of time. Diazo compound 2 had a vapor pressure of ~ 10 Torr and was diluted to 100 Torr with krypton or xenon in a 5-L storage bulb on the substrate rack. The krypton or xenon dilution of 2 was used to help eliminate Penning ionization of 2 or other reactant gases downstream of the ion production region by helium metastable atoms ($\text{He}^*(2^3\text{S})$) which are produced by the electron gun. These Penning processes could result in erroneous rate measurements (see below) because they yield electrons which can provide additional pathways for negative ion formation. The neutral reactants were loaded into 5-L bulbs either as the pure material (for slow reactions) or diluted with purified helium (for fast reactions).

Total reaction rate constants for the negative ion, I^- , generated in the ion preparation region of the flow tube were measured using standard pseudo-first-order kinetics and the fixed point observation method. The negative ion I^- will decay by diffusion to the walls, reaction with background impurities (or added substrate molecule), M, used to generate I^- , and reaction with the added reactant N. Since I^- is present in low concentration, the integrated rate law for these three processes is given by

$$\ln([\text{I}^-]/[\text{I}_0^-]) = \{(D_0/\Lambda^2 P_{\text{He}}) + k_{\text{M}}[\text{M}] + k_{\text{N}}[\text{N}]\}(z/v) \quad (1)$$

In eq 1, $[\text{I}_0^-]$ can be defined as the concentration of I^- as the flow passes the entrance port for N, and $[\text{I}^-]$ is the concentration at the first nose cone. Division of the flow distance, z , by the bulk flow velocity ($\sim 80 \text{ m s}^{-1}$ in our FA), v , gives the reaction time. It is evident that a plot of the logarithm of the mass spectrometer signal for I^- vs. $[\text{N}]$ should give a straight line with the slope $= k_{\text{N}}z/v$; see Figures 3 and 4. For our work, we assumed (and confirmed by testing with reactions of known rate constants) that the average transport velocity of the ions was the average buffer gas flow velocity multiplied by 1.59.¹⁴ The slopes of the log $[\text{I}^-]$

(13) The available ionizing energies of $\text{Kr}^*(^3\text{P}_2)$ and $\text{Xe}^*(^3\text{P}_2)$, should they be formed, are 9.9 and 8.3 eV, respectively, compared to 19.8 eV for $\text{He}^*(2^3\text{S})$: Moore, C. E. "Atomic Energy Levels," Vol. 1; U.S. Government Printing Office: Washington, D.C., 1949.

(14) Huggins, R. W.; Cahn, J. H. *J. Appl. Phys.* **1967**, *38*, 180.

vs. $[N]$ plots are converted to rate constants at 298 K using the equation

$$k \text{ (cm}^3 \text{ molecule}^{-1} \text{ s}^{-1}) = \frac{d(\log[I^-])}{d[N] \text{ (molecules cm}^{-3})} \times \frac{F_{\text{He}} \text{ (atm cm}^3 \text{ s}^{-1}) \times 2.78 \times 10^3 \text{ (torr atm}^{-1})}{P_{\text{He}} \text{ (torr)} \times \pi r^2 \text{ (cm)}^2 \times D \text{ (cm)}} \quad (2)$$

where the flow rate of N was converted to concentration by

$$[N] \text{ (molecules cm}^{-3}) = \frac{F_N \text{ (atm cm}^3 \text{ s}^{-1}) \times P_{\text{He}} \text{ (torr)}}{F_{\text{He}} \text{ (atm cm}^3 \text{ s}^{-1})} \times 3.26 \times 10^{16} \text{ (molecules cm}^{-3} \text{ torr}^{-1})$$

$[I^-]$ is the ion signal in arbitrary units, $[N]$ is the neutral reactant concentration, F_{He} and P_{He} are the flow and pressure of the helium buffer gas, respectively, r is the flow tube radius, and D is the distance of the neutral reactant inlet from the first nose cone. The constant in eq 2 contains the parabolic flow correction of 1.59.¹⁴

In order for the above formulation to be correct, it is essential that there be no formation steps for I^- after the gas flow passes the entrance port of N. We took special care to eliminate all processes (mainly $\text{He}^*(2^3\text{S})$ reactions) that might release electrons into this region of the flow and lead to further formation of I^- . As long as the diffusion and $k_M[M]$ loss terms are invariant with addition of N, these processes cause no difficulty in obtaining k_N .

The helium buffer gas pressure could be varied by altering the flow to the flow tube or by changing the pumping speed by a throttling valve. In the present experiments, pressures of ca. 0.5 torr were normally used, as measured by a calibrated 0–5 torr Celesco pressure transducer. In some cases, the pressure was increased to 1.4 torr to investigate the lack of effects of three-body collisions or whether certain product ions arise from primary ion-molecule reactions.

Mass spectra of the negative ions present in the flow before and after addition of the neutral reactant were taken. Nose cone and lens bias potential settings were adjusted to maximize ion signals. Usually a mass range from m/z 0 to 200 was taken initially, and then the range attenuated to include all ion signals (or as many as reasonable) for a kinetic run. Spectra are observed on an oscilloscope, and stored on disk and/or plotted on a Bascom-Turner electronic recorder; up to 16 separate spectra can be averaged on the recorder. We have found that identical bimolecular ion-molecule rate constants, within experimental error, were obtained using peak heights or integrated areas, or ion counting monitoring of a single ion. The convenience of measuring changes of ion signal peak heights of starting and product ions from the full spectral record as neutral reactant flow was varied was employed in these investigations.

To assess the accuracy of our rate-constant measurements, two known reaction rates for S_N2 displacement on methyl bromide by F^- (fast) and Cl^- (slow)¹⁵ were examined. For the reaction of $F^- + \text{CH}_3\text{Br} \rightarrow \text{Br}^- + \text{CH}_3\text{F}$, an average of $k = 1.6 \times 10^{-9} \text{ cm}^3 \text{ molecule}^{-1} \text{ s}^{-1}$ (standard deviation of 15%) compares favorably with the reported value ($k = 1.2 \times 10^{-9}$).¹⁵ For $Cl^- + \text{CH}_3\text{Br} \rightarrow \text{Br}^- + \text{CH}_3\text{Cl}$, our results give $k = 2.4 \times 10^{-11} \text{ cm}^3 \text{ molecule}^{-1} \text{ s}^{-1}$ (SD of 6%) from three experiments, in good agreement with the results of Bohme et al. (2.1×10^{-11}).¹⁵ These rate constants are within the experimental uncertainties of the two laboratories. In calculating these rate constants, fully developed parabolic flow was assumed; i.e., the plug flow velocity was multiplied by the 1.59 factor to get the true flow velocity.¹⁴

Gas purities and suppliers were helium (99.99%, Welder Products); krypton and xenon (Cryogenic Rare Gas Labs); ethylene (99.9%), ethylene oxide (99.7%), CH_3F (99%), CH_3Cl (99.5%), CH_3Br (99.5%), CH_4 (99.9%), N_2O (99%), NO_2 (99.5%), $\text{CH}_2=\text{CHCl}$, and $\text{c-C}_3\text{H}_6$ (99.9%) (Matheson); CF_4 and $\text{CH}_2=\text{CHF}$ (PCR); THF, CH_3OH , EtOH, n -PrOH, and t -BuOH (Fisher reagent grade); $(\text{CF}_3)_2\text{CHOH}$ (Du Pont); $\text{CF}_3\text{CH}_2\text{OH}$ (Halocarbon Products); $\text{CH}_2=\text{CHCN}$, $\text{CH}_2=\text{CHCO}_2\text{CH}_3$ (Eastman); CH_3OD (Merck); EtOD (Stohler); C_6F_6 (Aldrich). The alcohols were distilled and dried over molecular sieves. The alcohols, acrylonitrile, methyl acrylate, and C_6F_6 were transferred to their gas storage bulbs after three freeze-pump-thaw degassing cycles; the gases were used directly.

Diazocyclopentadiene (2). This diazo compound was prepared according to the procedure described by Doering and DePuy,¹⁶ bp 30 °C (30 torr), as a reddish liquid in ca. 40% yield. The IR and ^1H NMR spectra were compatible with this structure and indicated that no impurities were present.¹⁷ On one occasion, a 20-g sample of 2 exploded

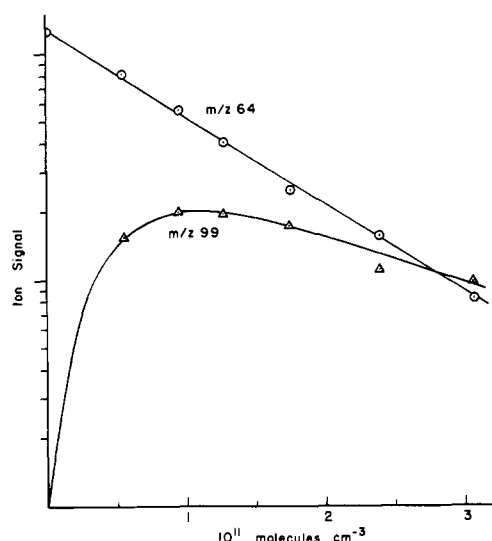


Figure 4. Semilogarithmic plot of decay of the parent ion and formation of $\text{CF}_3\text{CH}_2\text{O}^-$ for the reaction of **1** + $\text{CF}_3\text{CH}_2\text{OH}$. Ion signals are in arbitrary units. Formation of the cluster ion m/z 199 was omitted.

during an NMR sample preparation.

Results

The kinetic and product data for the ion-molecule reactions of carbene anion radical **1** are summarized in Table I. In the slow reaction of **1** with tetrahydrofuran (THF), which has the smallest IP of the neutrals studied, extra xenon ($2 \times 10^{13} \text{ molecules cm}^{-3}$) was added to the flow just downstream of the electron gun to ensure $\text{H}^*(2^3\text{S})$ destruction. Without this additional xenon, the signal of **1** increased somewhat with the first increments of THF. Since this reaction is slow, large concentrations of THF were added to observe only small changes in the ion signal of **1**. Apparently, the xenon used in diluting **2** did not completely remove $\text{He}^*(2^3\text{S})$ and Penning ionization of THF gave secondary electrons which attached to molecules of **2**. This precaution was taken whenever necessary with other slow reactions and neutral reactants with low IPs.

In all cases, clean pseudo-first-order decay plots of the ion signal of **1** (m/z 64) vs. concentrations of neutral reactant were observed. A typical semilogarithmic plot is shown in Figure 3 for the reaction of **1** with ethylene oxide, which is a slow reaction. The results of the fast protonation of **1** by $\text{CF}_3\text{CH}_2\text{OH}$ are shown in Figure 4. These figures display the range of reactant concentrations that were typically used. The product ion distributions are the relative ion signals observed from the mass spectrometer.

Discussion

Generation of Cyclopentadienylidene Anion Radical (1). Two methods were considered for generating **1** (C_5H_4^-): (a) dissociative attachment of a thermal electron to diazocyclopentadiene (**2**) and (b) reaction of cyclopentadiene with O^- .¹⁸ Method (a) should be less exoergic giving a greater probability that the m/z 64 anion would have the structure of **1**. When a small flow ($\sim 10^{10} \text{ molecules cm}^{-3}$) of **2** was added to the helium gas flow upstream of the electron gun, the only two anions observed were m/z 64 (M^-) and 65 ($\text{M} + 1$); the relative intensity was 1/0.055, which agrees with the theoretical $\text{M}/(\text{M} + 1)$ value of 1/0.055.¹⁹

Reactions of 1 with 2. Comparisons with Solution Data. Increasing the flow of diazo compound **2**, added before the electron gun, to $\sim 5 \times 10^{11} \text{ molecules cm}^{-3}$ produced an initial increase followed by a decrease in the m/z 64 signal, appearance of a new strong signal at m/z 156, $\text{C}_{10}\text{H}_8\text{N}_2^-$ (m/z 157 ($\text{M} + 1$); 158 ($\text{M} + 2$); obsd. 1:0.116:0.004, theory 1:0.117:0.006),¹⁹ and a relatively weaker signal at m/z 128, $\text{C}_{10}\text{H}_8^-$ (m/z 129 ($\text{M} + 1$); obsd.

(15) Tanaka, K.; Mackay, G. I.; Payzant, J. D.; Bohme, D. K. *Can. J. Chem.* **1976**, *54*, 1643.

(16) Doering, W. von E.; DePuy, C. H. *J. Am. Chem. Soc.* **1953**, *75*, 5955.

(17) We thank Kevin Reid for preparation of **2**.

(18) Domenico, A. di; Harland, P. W.; Franklin, J. L. *J. Chem. Phys.* **1972**, *56*, 5299.

(19) Beynon, J. H.; Williams, A. E. "Mass and Abundance Tables for Use in Mass Spectrometry"; American Elsevier: New York, 1963.

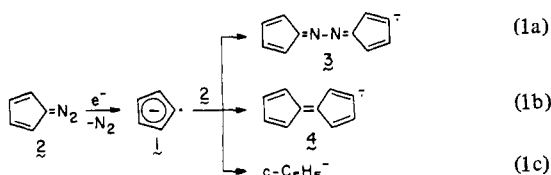
Table I. Summary of Kinetic and Product Data for the Ion-Molecule Reactions of Cyclopentadienylidene Anion Radical (1)

rxn	ion + neutral reactants	products [assumed neutral]	fraction of product ion signal	k_{total}^a , $\text{cm}^3 \text{ molecule}^{-1} \text{ s}^{-1}$
1a	1 + (c-C ₅ H ₄)=N ₂	→ (c-C ₅ H ₄)=NN=(c-C ₅ H ₄) ⁻ ·	0.64	(4.4 ± 0.4)10 ⁻¹⁰
1b		→ (c-C ₅ H ₄)=NN=(c-C ₅ H ₄) ⁻ ·[+N ₂]	0.22	
1c		→ c-C ₅ H ₅ ⁻ ·	0.14	
2a	1 + CH ₃ OH	→ c-C ₅ H ₅ ⁻ ·[+CH ₃ O·]	1.00	(8.3 ± 0.3)10 ⁻¹⁰
2b	1 + CH ₃ OD	→ c-C ₅ H ₄ D ⁻ ·	0.96	
2c		→ c-C ₅ H ₅ ⁻ ·	0.04	
3a	1 + CH ₃ CH ₂ OH	→ c-C ₅ H ₅ ⁻ ·[+CH ₃ CH ₂ O·]	0.83	(7.1 ± 0.1)10 ⁻¹⁰
3b		→ CH ₃ CH ₂ O ⁻ ·[+c-C ₅ H ₅ ·]	0.17	
3c	1 + CH ₃ CH ₂ OD	→ c-C ₅ H ₄ D ⁻ ·	0.95	
3d		→ c-C ₅ H ₅ ⁻ ·	0.05	(6.1 ± 0.6)10 ⁻¹⁰
4a	1 + CH ₃ (CH ₂) ₂ OH	→ c-C ₅ H ₅ ⁻ ·[+CH ₃ (CH ₂) ₂ O·]	0.65	
4b		→ CH ₃ (CH ₂) ₂ O ⁻ ·[+c-C ₅ H ₅ ·]	0.35	
5a	1 + (CH ₃) ₃ COH	→ c-C ₅ H ₅ ⁻ ·[+(CH ₃) ₃ CO·]	0.21	(6.7 ± 0.1)10 ⁻¹⁰
5b		→ (CH ₃) ₃ CO ⁻ ·[+c-C ₅ H ₅ ·]	0.79	
6	1 + CF ₃ CH ₂ OH	→ CF ₃ CH ₂ O ⁻ ·[+c-C ₅ H ₅ ·]	1.00	
7	1 + (CF ₃) ₂ CHOH	→ (CF ₃) ₂ CHO ⁻ ·[+c-C ₅ H ₅ ·]	1.00	(1.2 ± 0.1)10 ⁻⁹
(see text for anion-cluster formation by alcohols in reactions 3-7)				
8	1 + THF	→ c-C ₅ H ₅ ⁻ ·[+α-tetrahydrofuryl] ^b	1.00	(1.2 ± 0.1)10 ⁻¹¹
9	1 + H ₂ C=CH ₂	→ no rxn obsd		≤10 ⁻¹³
10	1 + c-C ₃ H ₆	→ no rxn obsd ^b		≤10 ⁻¹³
11	1 + CH ₄	→ no rxn obsd		≤10 ⁻¹³
12	1 + CH ₃ F	→ no rxn obsd		≤10 ⁻¹³
13a	1 + CH ₃ Cl	→ c-C ₅ H ₅ ⁻ ·[+·CH ₂ Cl]	0.99	(8.8 ± 0.2)10 ⁻¹²
13b		→ Cl ⁻ [+c-C ₅ H ₄ CH ₃ ·]	0.01	
14a	1 + CH ₃ Br	→ Br ⁻ [+(c-C ₅ H ₄)CH ₃ ·]	0.81	
14b		→ c-C ₅ H ₅ ⁻ ·[+·CH ₂ Br]	0.19	(1.3 ± 0.1)10 ⁻¹⁰
15a	1 + H ₂ C=COCH ₂	→ c-C ₅ H ₅ ⁻ ·[+C ₂ H ₃ O·]	0.49	(9.5 ± 0.7)10 ⁻¹³
15b		→ H ₂ C=CHO ⁻ ·[+c-C ₅ H ₅ ·]	0.37	
15c		→ C ₆ H ₆ O ⁻ ·[+CH ₂ ·]	0.08	
15d		→ c-C ₅ H ₄ CH ₂ O ⁻ ·	0.06	(8.2 ± 0.1)10 ⁻¹⁰
16a	1 + CH ₂ =CHCN	→ c-C ₅ H ₄ CH=CHCN ⁻ ·[+H·]	0.31	
16b		→ CN ⁻ [see text]	0.57	
16c		→ m/e 52	0.10	
16d		→ c-C ₅ H ₅ ⁻ ·[+C ₃ H ₂ N·]	0.02	
17a	1 + CH ₂ =CHCO ₂ CH ₃	→ c-C ₅ H ₄ CH=CHCO ₂ CH ₃ ⁻ ·[+H·]	0.74	(1.1 ± 0.1)10 ⁻¹⁰
17b		→ c-C ₅ H ₅ ⁻ ·[+C ₄ H ₅ O ₂ ·]	0.26	
18a	1 + CH ₂ =CHCl	→ Cl ⁻ [see text]	0.88	
18b		→ c-C ₅ H ₅ ⁻ ·[+C ₂ H ₂ Cl·]	0.12	(2.3 ± 0.1)10 ⁻¹¹
19	1 + CH ₂ =CHF	→ no rxn obsd		≤10 ⁻¹³
20	1 + N ₂ O	→ no rxn obsd		≤10 ⁻¹³
21a	1 + NO ₂	→ NO ₂ ⁻ ·[+c-C ₅ H ₄ ·]	0.68	(5.7 ± 0.1)10 ⁻¹⁰
21b		→ c-C ₅ H ₄ NO ₂ ⁻ ·	0.29	
21c		→ c-C ₅ H ₄ O ⁻ ·[+NO]	0.03	
22	1 + C ₆ F ₆	→ c-C ₅ H ₄ C ₆ F ₅ ⁻ ·[+F·]	1.00	rate not measured

^a k 's are estimated to be accurate to ±30%. Errors given are standard deviations from multiple determinations. To convert to units of L mol⁻¹ s⁻¹ multiply by 6 × 10²⁰ molecules L mol⁻¹ cm⁻³. To obtain the rate constant of a particular reaction channel multiply the fraction of the product ion signal by k . ^b In these reactions 2 × 10¹³ molecules cm⁻³ of Xe was added at the stationary port downstream of the electron gun to ensure He*(2³S) destruction before the flow reached the port for neutral addition.

1:0.112, theory 1:0.109),¹⁹ and an increase in the signal at m/z 65 (m/z 66 (M + 1); obsd. 1:0.057, theory 1:0.055).¹⁹ The rate constant for the reaction of 1 + 2 and the branching ratios for these three reaction channels (reactions 1a–c, Table I) were then determined by adding 2 through the inlet ca. 30 cm downstream from the electron gun. Changes in the helium pressure from 0.4 to 1.3 torr did not alter the relative ion signals for m/z 65, 128, and 156, indicating that each was a primary product in the reaction of 1 + 2.

These observations are consistent with 1 (a) adding to the terminal nitrogen (N₅) of 2 giving cyclopentadienone azine anion radical, C₁₀H₈N₂⁻· (3, reaction 1a), (b) adding to C₁ of 2 and loss of nitrogen giving pentafulvalene anion radical, C₁₀H₈⁻· (4, reaction 1b), and (c) abstracting H- from 2 to yield cyclopentadienyl anion, c-C₅H₅⁻ (reaction 1c). Each of these three reaction channels has



condensed- and/or gas-phase analogies. In solution, electro-

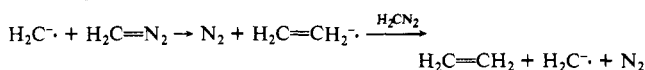
chemical and chemical reductions of diaryldiazomethanes to the corresponding carbene anion radicals yield azine anion radicals^{2,3} or their further reduction products¹ as major products. Vinylidene anion radical (H₂C=C⁻·) was recently shown to add nucleophilically to N₅ of N₂O,^{20,21} a compound which is isoelectronic with diazomethane. Reaction b is analogous to the formation of olefins from triplet methylenes reacting with diazoalkanes.^{22,23} Reaction c illustrates a "normal" reaction, H- abstraction, of radical species with C-H containing organic compounds. Since k for reaction 1 was rather large, only limited amounts of 2 can

(20) Dawson, J. H. J.; Nibbering, N. M. M. *J. Am. Chem. Soc.* **1978**, *100*, 1928.

(21) Bierbaum, V. M.; DePuy, C. H.; Shapiro, R. H. *J. Am. Chem. Soc.* **1977**, *99*, 5800.

(22) (a) Jones, M.; Moss, R. A., Eds. "Carbenes"; Wiley-Interscience: New York, 1973, 1975; Vol. 1, 2. (b) Kirmse, W. "Carbene Chemistry", 2nd ed.; Academic Press: New York, 1971.

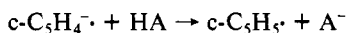
(23) Ethylene has been found to be the major gas reduction product from CH₂N₂ with excess sodium naphthalene in THF: McDonald, R. N.; Singh, B. P., unpublished results. It is considered that the reaction



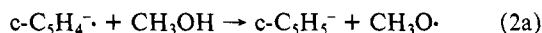
is a reasonable pathway to the olefin.²⁴

be added to the flow before the electron gun to retain a reasonable signal for anion **1** in the reaction zone of the FA.

Protonation of Anion Radical 1. Determination of the proton affinity (PA) of the $c\text{-C}_5\text{H}_4^-$ species produced by dissociative electron attachment with **2** is required for various thermochemical considerations. It would also allow us to determine whether the $\sigma^1\pi^2$ (**1**) or the $\sigma^2\pi^1$ electronic configuration is the ground state of this anion radical. The $\sigma^2\pi^1$ electronic configuration of $c\text{-C}_5\text{H}_4^-$ would be similar in several respects to that of the phenyl anion (PA(C_6H_5^-) = 398 ± 7 kcal mol $^{-1}$)²⁵ and similar PAs would be expected. The product of protonation of $c\text{-C}_5\text{H}_4^-$ will be the cyclopentadienyl radical, $c\text{-C}_5\text{H}_5^\cdot$.

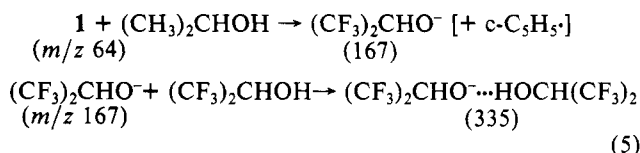


The first potential proton donor HA investigated was CH_3OH ($\Delta H^\circ_{\text{acid}}(\text{CH}_3\text{OH}) = 379 \pm 2$ kcal mol $^{-1}$).²⁵ While a fast reaction between $c\text{-C}_5\text{H}_4^-$ and CH_3OH was observed, CH_3O^- or its cluster ions, $\text{CH}_3\text{O}^-(\text{HOCH}_3)_n$, were not observed as product ions. The only anionic reaction product was $c\text{-C}_5\text{H}_5^-$ (Table I, reaction 2a) formed by H \cdot abstraction by $c\text{-C}_5\text{H}_4^-$ from CH_3OH . The fact that CH_3OH failed to protonate $c\text{-C}_5\text{H}_4^-$ requires that this anion radical has the ground state $\sigma^1\pi^2$ electronic configuration as shown in **1**.

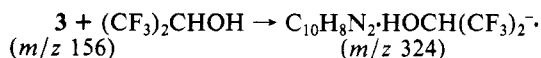


Initially, the H \cdot source in this reaction was considered to be the C-H bond ($D^\circ(\text{HOCH}_2\text{-H}) = 95.9$ kcal mol $^{-1}$)²⁶ rather than the O-H bond ($D^\circ(\text{CH}_3\text{O-H}) = 104 \pm 1$ kcal mol $^{-1}$).²⁷ However, the reaction of $c\text{-C}_5\text{H}_4^-$ with CH_3OD (99% d_1) showed that the anion product was $c\text{-C}_5\text{H}_4\text{D}^-$ (reaction 2b). The 4% of $c\text{-C}_5\text{H}_5^-$ formed (reaction 2c) probably arises from CH_3OH formed by D-H exchange in the glass storage bulb. This same result was found using $\text{CH}_3\text{CH}_2\text{OD}$ (reactions 3c,d). This large $k_{\text{OH}}/k_{\text{CH}} \geq 24$ H \cdot abstraction ratio is somewhat greater than that of methyl radical reacting with methanol in the gas phase ($k_{\text{OH}}/k_{\text{CH}} \approx 16$),²⁸ in solution, $k_{\text{OH}}/k_{\text{CH}} \approx 0.02$.²⁹

Turning to the stronger acids $(\text{CF}_3)_2\text{CHOH}$ ($\Delta H^\circ_{\text{acid}} < 351$ kcal mol $^{-1}$)²⁵ and $\text{CF}_3\text{CH}_2\text{OH}$ ($\Delta H^\circ_{\text{acid}} = 364.4 \pm 2$ kcal mol $^{-1}$),²⁵ both alcohols produced *only* protonation (reactions 6 and 7). The fast protonation reaction between **1** and $(\text{CF}_3)_2\text{CHOH}$ was accompanied by formation of three negative ion products, m/z 167 (m/z 168 (M + 1); obsd. 1:0.037, theory 1:0.032),¹⁹ 324, and 335.

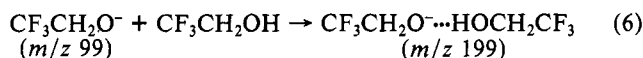
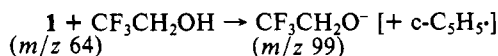


No increase in m/z 65 was observed verifying that H \cdot abstraction from $(\text{CF}_3)_2\text{CHOH}$ by **1** had not occurred. The anions at m/z 167 and 335 are the alkoxide, $(\text{CF}_3)_2\text{CHO}^-$, and its alcohol cluster, respectively. The products of this reaction were further complicated by formation of a small amount of an anion m/z 324 at large flows of $(\text{CF}_3)_2\text{CHOH}$. While this signal was too small to accurately determine the $M/(M + 1)$ ratio, it corresponds to reaction of the alcohol with the azine anion radical **3**.



Development of the m/z 324 anion signal was associated with decay of the signal of **3**.

Similar results were obtained from the reaction of **1** with $\text{CF}_3\text{CH}_2\text{OH}$ (Figure 4). The anion product $\text{CF}_3\text{CH}_2\text{O}^-$ was observed at m/z 99 (m/z 100 (M + 1); obsd. 1:0.025, theory 1:0.023)¹⁹ with anion cluster formation occurring at larger flows of $\text{CF}_3\text{CH}_2\text{OH}$. No reaction of azine anion radical **3** with $\text{CF}_3\text{CH}_2\text{OH}$ was observed.



The reaction of **1** with $(\text{CH}_3)_3\text{COH}$ ($\Delta H^\circ_{\text{acid}} = 373.3 \pm 2$ kcal mol $^{-1}$)²⁵ proceeded by two reaction channels, protonation and H \cdot abstraction (reactions 5a,b), with $k_{\text{H}}/k_{\text{H}} = 3.8$. The two product anions were $c\text{-C}_5\text{H}_5^-$ (m/z 65) and $(\text{CH}_3)_3\text{CO}^-$ (m/z 73; m/z 74 (M + 1), obsd. 1:0.046, theory 1:0.045),¹⁹ and minor cluster formation $(\text{CH}_3)_3\text{CO-HOC}(\text{CH}_3)_3$ (m/z 147). Again, no reaction of **3** with $(\text{CH}_3)_3\text{COH}$ was observed. We assume that H \cdot abstraction occurred from the O-H bond.

Both reaction channels, protonation and H \cdot abstraction, were observed in the reaction of **1** with $\text{CH}_3(\text{CH}_2)_2\text{OH}$ ($\Delta H^\circ_{\text{acid}} = 374.7$ kcal mol $^{-1}$)²⁵ with $k_{\text{H}}/k_{\text{H}} = 0.54$ (reactions 4a,b). The anion products were $c\text{-C}_5\text{H}_5^-$ (m/z 65), $\text{CH}_3(\text{CH}_2)_2\text{O}^-$ (m/z 59; m/z 60 (M + 1), obsd. 1:0.032, theory 1:0.034),¹⁹ and two cluster ions, $\text{CH}_3(\text{CH}_2)_2\text{O-HO}(\text{CH}_2)_2\text{CH}_3$ (m/z 119) and $\text{CH}_3(\text{CH}_2)_2\text{O}^-(\text{H-O}(\text{CH}_2)_2\text{CH}_3)_2$ (m/z 179). We assume that H \cdot abstraction occurred from the O-H bond.

A tighter bracket on the PA(**1**) was achieved in the reaction of **1** with $\text{CH}_3\text{CH}_2\text{OH}$ ($\Delta H^\circ_{\text{acid}} = 376.1 \pm 2$ kcal mol $^{-1}$)²⁵ where the ratio $k_{\text{H}}/k_{\text{H}} = 0.20$ is the smallest observed value (reactions 3a,b). The anion products were $c\text{-C}_5\text{H}_5^-$ (m/z 65), $\text{CH}_3\text{CH}_2\text{O}^-$ (m/z 45; m/z 46 (M + 1), obsd. 1:0.022, theory 1:0.023),¹⁹ and two cluster ions, $\text{CH}_3\text{CH}_2\text{O-HOCH}_2\text{CH}_3$ (m/z 91) and $\text{CH}_3\text{CH}_2\text{O}^-(\text{HOCH}_2\text{CH}_3)_2$ (m/z 137). The reaction of **1** with $\text{CH}_3\text{C-H}_2\text{OD}$ (reactions 3c,d) again established that H \cdot abstraction by **1** occurred from the O-H(D) bond of the alcohol.

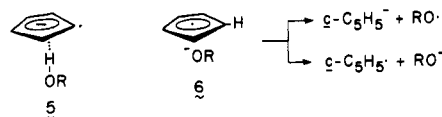
Extrapolation of the rate constants for protonation of **1** by these three alcohols on the Bartmess-McIver scale²⁵ gives PA(**1**) = 377 ± 2 kcal mol $^{-1}$. From the relationship

$$\Delta H_f^\circ(\text{1}) = \text{PA}(\text{1}) + \Delta H_f^\circ(c\text{-C}_5\text{H}_5^-) - \Delta H_f^\circ(\text{H}^+)$$

we calculate $\Delta H_f^\circ(\text{1}) = 70.7 \pm 3.2$ kcal mol $^{-1}$ at 298 K, using $\Delta H_f^\circ(c\text{-C}_5\text{H}_5^-) = 60.9 \pm 1.2$ ³⁰ and $\Delta H_f^\circ(\text{H}^+) = 367.2$ kcal mol $^{-1}$.³¹

It is interesting to note that PA(**1**) is greater than PA($c\text{-C}_5\text{H}_5^-$) (356.1 ± 2 kcal mol $^{-1}$)²⁵ by ca. 21 ± 4 kcal mol $^{-1}$. The principal reason for this is that the product from **1** plus a proton is $c\text{-C}_5\text{H}_5^\cdot$ ($\Delta H_f^\circ(c\text{-C}_5\text{H}_5^\cdot) - \Delta H_f^\circ(\text{1}) \sim -10$ kcal mol $^{-1}$)³⁰ while the protonation product from $c\text{-C}_5\text{H}_5^-$ is cyclopentadiene ($\Delta H_f^\circ(c\text{-C}_5\text{H}_6) - \Delta H_f^\circ(c\text{-C}_5\text{H}_5^-) \sim +11$ kcal mol $^{-1}$).²⁵ These same factors, although smaller in magnitude, account for the increased nucleophilicity of **1** compared to $c\text{-C}_5\text{H}_5^-$.^{32b}

To account for the large $k_{\text{OH}}/k_{\text{CH}}$ H \cdot abstraction ratios by **1** with CH_3OH and $\text{CH}_3\text{CH}_2\text{OH}$ (assumed also for $n\text{-PrOH}$ and $t\text{-BuOH}$) and the large rate constants for such H \cdot abstraction reactions compared to other H \cdot donors (see below), we suggest that these reactions of **1** with alcohols proceed via a hydrogen-bonded anion-alcohol complex **5**.^{32c} The competition between



(24) Sargent, G. D.; Tatum, C. M.; Scott, R. P. *J. Am. Chem. Soc.* **1974**, *96*, 1602.

(25) Bartmess, J. E.; McIver, R. T. In "Gas Phase Ion Chemistry", Bowers, M. T., Ed.; Academic Press: New York, 1979; Vol. 2.

(26) O'Neal, H. E.; Benson, S. W. In "Free Radicals", Kochi, J. K., Ed.; Wiley: New York, 1973; Vol. 2.

(27) (a) Benson, S. W.; Cruickshank, F. R.; Golden, D. M.; Haugen, G. R.; O'Neal, H. E.; Rogers, A. S.; Shaw, R.; Walsh, R. *Chem. Rev.* **1969**, *69*, 279. (b) Engelking, P. C.; Ellison, G. B.; Lineberger, W. C. *J. Chem. Phys.* **1978**, *69*, 1826, report $\Delta H_f^\circ(\text{CH}_3\text{O}^-) = 0.7 \pm 1.0$ kcal mol $^{-1}$.

(28) Shannon, T. W.; Harrison, A. G. *Can. J. Chem.* **1963**, *41*, 2455.

(29) Char, M. *J. Phys. Chem.* **1963**, *67*, 605.

(30) Furuyama, S.; Golden, D. M.; Benson, S. W. *Int. J. Chem. Kinet.* **1971**, *3*, 237.

(31) "JANAF Thermochemical Tables", *Natl. Stand. Ref. Data Ser., Natl. Bur. Stand.* **1971**, No. 37.

(32) McDonald, R. N.; Chowdhury, A. K.; Setser, D. W., unpublished FA results. (a) $c\text{-C}_5\text{H}_5^- + (\text{CF}_3)_2\text{CHOH} \rightarrow k = (1.3 \pm 0.1) \times 10^{-9}$ cm 3 molecule $^{-1}$ s $^{-1}$. $c\text{-C}_5\text{H}_5^- + \text{CF}_3\text{CH}_2\text{OH} \rightarrow k = (3.1 \pm 0.1) \times 10^{-10}$ cm 3 molecule $^{-1}$ s $^{-1}$. (b) Rate increases of 50–100 are observed for nucleophilic ion-molecule reactions of **1** compared to those of $c\text{-C}_5\text{H}_5^-$. (c) We have observed formation of the $c\text{-C}_5\text{H}_5^-\text{HOCH}_2\text{CF}_3$ cluster (*J. Am. Chem. Soc.*, **1980**, *102*, 4836).

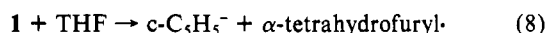
Table II. Substituent Effects on H• Abstraction by **1** on Substituted Ethylenes

rxn	CH ₂ =CHX substituent	<i>k</i> _{abstraction} ^a cm ³ molecule ⁻¹ s ⁻¹
16d	CN	~1.6 × 10 ⁻¹¹
17b	CO ₂ CH ₃	2.9 × 10 ⁻¹¹
18b	Cl	2.8 × 10 ⁻¹²
19	F	≤10 ⁻¹³
9	H	≤10 ⁻¹³

protonation vs. H• abstraction from **5** depends on the *D*^o of the complexed OH bond and the PA of RO⁻. A more detailed mechanistic view could involve the ion-radical pair **6** produced by ring protonation from **5**. The outcome of decomposition of ion-radical pair **6** would then depend on the relative electron affinities (EA) of RO• and c-C₅H₅•,³³ as well as details of the potential surfaces associated with the two exit channels.

Hydrogen Atom Abstraction Reactions of 1. This classic reaction of organic free radicals was probed not only to establish this reaction channel, but also to gain thermochemical information about **1** and certain related species. In Table I, hydrogen-atom abstraction was observed for all reactions of **1** with reactants containing hydrogens except those with the fluorinated alcohols, reactions 6 and 7. The rate constants for H• abstraction range from 8.3 × 10⁻¹⁰ cm³ molecule⁻¹ s⁻¹ for methanol (reaction 2) to ~5 × 10⁻¹³ molecule⁻¹ s⁻¹ for ethylene oxide (reaction 15a). The anion product of these reactions is the π-delocalized anion c-C₅H₅⁻. Except for the reaction with methanol, the *k*'s for H• abstraction by **1** are ≤3 × 10⁻¹¹ cm³ molecule⁻¹ s⁻¹.

Attempts to establish the upper limit on the H• affinity of **1** using H₂C=CH₂ (*D*^o(H₂CCH-H) ≥ 108 kcal mol⁻¹),²⁶ c-C₅H₆ (*D*^o(c-C₅H₅-H) = 106.3 ± 0.25 kcal mol⁻¹),³⁵ and CH₄ (*D*^o(H₃C-H) = 104.9 ± 0.15 kcal mol⁻¹)³⁶ failed; no reaction between **1** and these reactants was observed (reactions 9–11). The two factors influencing the failure to observe these H• transfers are (a) the H• transfer is truly endoergic, or (b) there is a ≥3 kcal mol⁻¹ barrier to these H• abstraction reactions.³⁷ The presence of a 1–2 kcal mol⁻¹ barrier in the reaction



explains why **1** with THF exhibits a slow H• transfer rate, although the reaction is reasonably exoergic (*D*^o(α-tetrahydrofuryl-H) = 91.8 kcal mol⁻¹).²⁶ This also appears to be the case with the slow H• transfers between **1** and CH₃Cl and CH₃Br (reactions 13a and 14b) and accounts for the fact that no reaction was observed with **1** and CH₃F even though ion-dipole interactions will exist in these collision pairs.

Formation of the hydrogen-bonded complex **5** between **1** and ROH could reduce or eliminate such barriers. Using the reactions of **1** with CH₃OH or CH₃CH₂OH where H• abstraction was shown to occur from the OH bond, we calculate Δ*H*_f^o(**1**) ≥ 67.7 ± 3 kcal mol⁻¹ based on reactions 2a and 3a of Table I.^{27,38} Although this is a lower limit as determined from H• affinity bracketing of **1**, it is probably very close to the true value.

The H• abstraction reactions by **1** from the series of ethylenes (reactions 16d, 17b, 18b, 19, and 20) showed a marked substituent effect (Table II). Omitting reaction 17b from our considerations since H• abstraction from methyl acrylate may occur from the

Table III. Substituent Effects on H• Abstraction and Nucleophilic Substitution by **1** on CH₃X

rxn ^b	X	<i>k</i> _{abstraction} ^a	<i>k</i> _{substitution} ^a
14	Br	2 × 10 ⁻¹¹	1 × 10 ⁻¹⁰
13	Cl	9 × 10 ⁻¹²	~10 ⁻¹³
12	F	≤10 ⁻¹³	≤10 ⁻¹³

^a In units of cm³ molecule⁻¹ s⁻¹. ^b From Table I.

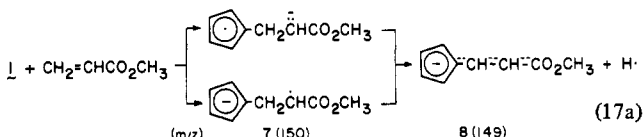
OCH₃ group, we find that the activating substituent influence is CN > Cl > F ≥ H. This progression appears to be more in line with H• abstraction from C_α-H of the olefin rather than from C_β-H.

Reactions of 1 with Methyl Halides. The reactions of **1** with three methyl halides (CH₃F, CH₃Cl, and CH₃Br) were examined. From the reaction of **1** with CH₃Br, the major reaction channel was nucleophilic displacement producing Br⁻ (reaction 14a) along with some H• abstraction (reaction 14b) yielding c-C₅H₅⁻. The reaction of **1** and CH₃Cl occurred by almost exclusive H• abstraction (reaction 13a). No ion-molecule reaction was observed for the reaction of **1** with CH₃F.

The rate constants for H• abstraction (Table III) by **1** from CH₃X suggest that *D*^o(H₂FC-H) > *D*^o(H₂ClC-H) ~ *D*^o(H₂BrC-H) by about 2–3 kcal mol⁻¹,³⁹ assuming similar activation energies for all three reactions. The rate constants for nucleophilic substitution for CH₃X by **1** follow the corresponding *D*^o(H₃C-X) values.^{32b,39}

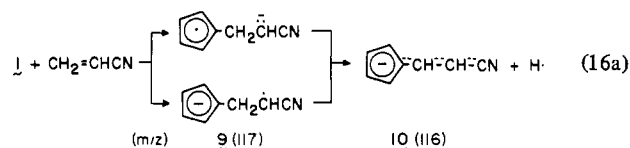
Reactions of 1 with Olefins. **1** failed to react with ethylene by either addition or H• abstraction. Failure to observe addition of **1** to ethylene was not too surprising based on the rates of addition of methyl, ethyl, and various other organic radicals with ethylene at elevated temperatures.^{40,41}

Reaction of **1** with methyl acrylate (reaction 17) occurred to yield two product anions, c-C₅H₅⁻ (*m/z* 65) and *m/z* 149 (*m/z* 150 (M + 1); obsd. 1:0.096, theory 1:0.099),¹⁹ C₉H₉O₂⁻. The latter anion is considered to result from addition of **1** to methyl acrylate followed by loss of H• producing delocalized anion **8**. In principle,



the addition reactions of **1** with H₂C=CHX could occur by either an anionic or radical mechanism shown with the two structures of **7** (also **9** and **13**).

The reaction of **1** with acrylonitrile was more complicated, although a major reaction channel was formation of *m/z* 116 (*m/z* 117 (M + 1); obsd. 1:0.086, theory 1:0.091),¹⁹ C₈H₆N⁻ (reaction 16a). Two minor processes were formation of anions c-C₅H₅⁻ (*m/z* 65) and *m/z* 52 (too small for accurate (M + 1) determination). The *m/z* 52 anion was thought to be C₃H₂N⁻ formed by deprotonation of acrylonitrile by **1**. From simple considerations of cyano group interactions, this anion is considered to be the vinyl anion H₂C=CCN⁻ (**11**) rather than its C_β anionic isomer.⁴²



Formation of the principal product anion CN⁻ (*m/z* 26; *m/z* 27 (M + 1); obsd. 1:0.012, theory 1:0.015)¹⁹ can occur from several sources: (a) decomposition of excited **9*** or (b) **11***, or (c) by vicinal elimination of HCN from acrylonitrile. Increasing the

(33) For the components of the ion-radical pair **6** (kcal mol⁻¹): EA(c-C₅H₅•) = 41.2 ± 0.5;³⁴ EA(CH₃O•) = 39.4 ± 1.4, 36.2 ± 0.7;²⁵ EA(EtO•) = 39.8 ± 0.7;²⁵ EA(*n*-PrO•) = 41.2 ± 0.7;²⁵ EA(*t*-BuO•) = 44.8 ± 0.1, 43.8 ± 0.7.²⁵

(34) Engelking, P. C.; Lineberger, W. C. *J. Chem. Phys.* **1977**, *67*, 1412.

(35) Baghal-Vayjooee, M. H.; Benson, S. W. *J. Am. Chem. Soc.* **1979**, *101*, 2838.

(36) Baghal-Vayjooee, M. H.; Colussi, A. J.; Benson, S. W. *J. Am. Chem. Soc.* **1978**, *100*, 3214.

(37) Such barriers to H• abstraction processes by carbon radicals are not uncommon; Trotman-Dickenson, A. F.; Milne, G. S. "Tables of Bimolecular Gas Reactions", *Natl. Stand. Ref. Data Ser., Natl. Bur. Stand.* **1967**, No. 9.

(38) This result uses Δ*H*_f^o(c-C₅H₅•) = 19 ± 2 kcal mol⁻¹ from ref 18; ref 25 gives Δ*H*_f^o(c-C₅H₅•) = 21.3 ± 3 kcal mol⁻¹.

(39) Furuyama, S.; Golden, D. M.; Benson, S. W. *J. Am. Chem. Soc.* **1969**, *91*, 7564.

(40) Kerr, J. A.; Parsonage, M. J. "Evaluated Kinetic Data on Gas Phase Addition Reactions"; Butterworths: London, 1972.

(41) Tedder, J. M.; Walton, J. C. *Adv. Phys. Org. Chem.* **1978**, *16*, 51.

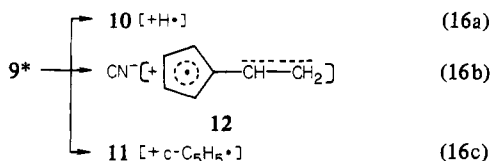
(42) Schmidt, R. R.; Talbiersky, J.; Russegger, P. *Tetrahedron Lett.* **1979**, 4273, and references cited therein.

Table IV. Summary of Data for Reactions of 1 with $\text{CH}_2=\text{CHX}$

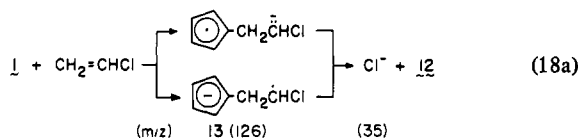
CH ₂ =CHX substituent	<i>k</i> ^a for adduct formation	<i>k</i> / <i>k</i> _E ^b	σ _p
CN	7 × 10 ⁻¹⁰	≥7000	0.660
CO ₂ CH ₃	1 × 10 ⁻¹⁰	≥1000	0.450
Cl	2 × 10 ⁻¹¹	≥200	0.227
F	≤10 ⁻¹³		0.062
H	≤10 ⁻¹³		0.000

^a In units of cm³ molecule⁻¹ s⁻¹ at 298 K. ^b K_E is the rate constant for ethylene + 1; k 's were invariant with pressure change (0.4–1.1 torr).

helium flow pressure in the reaction tube from 0.4 to 0.9 torr resulted in decreases in both CN^- and **11** while the signal for **10** increased. This pressure dependency indicated that formation of CN^- and **11** results from decomposition reactions of intermediates rather than being formed in primary processes. From these results, we conclude that the reaction of **1** + $\text{CH}_2=\text{CHCN}$ proceeds primarily to form **9*** which fragments by channels 16b and 16c. Channel 16b involves loss of CN^- with probably hydrogen migration to produce the π -delocalized vinylcyclopentadienyl radical (**12**), while channel 16c would require vicinal loss of $\text{c-C}_3\text{H}_5\cdot$ to yield anion **11**.



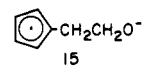
The reaction of **1** with vinyl chloride yielded primarily Cl^- (m/z 35 and 37, obsd. 1:0.33, theory 1:0.33). We consider this to be related to channel 16b with **1** adding to vinyl chloride yielding an excited adduct **13***. Since the $\text{C}_\alpha\text{-Cl}$ is less stabilizing than $\text{C}_\alpha\text{-CN}$ to either an α -anion⁴² or an α -radical center (σ constants), only reaction channel 18a was observed. Increasing the helium pressure did not alter the negative ion spectrum of this reaction (18a + 18b). No reaction was observed between **1** and vinyl fluoride under these conditions.



Based on the above discussion, the data for the reactions of **1** with the substituted ethylenes is summarized in Table IV. It is obvious that there is a strong substituent effect on these addition reactions of **1** + CH₂=CHX. The three measured values (X = CN, CO₂CH₃, Cl) are correlated using Hammett's σ_p constants giving $\rho = +4$. However, this magnitude of ρ is actually too small since it predicts $k \approx 10^{12}$ cm³ molecule⁻¹ s⁻¹ for vinyl fluoride and ethylene. Since the magnitudes of the measured substituent effects are far greater than those associated with gas-phase addition of radicals to such olefins,^{40,41} we conclude that these olefin additions by **1** proceed by a Michael (nucleophilic) addition process rather than by radical addition.

Reaction of 1 with Ethylene Oxide and Nitrous Oxide. Since the PA(1) was found to be only 2 kcal mol⁻¹ less than the PA(CH₃O⁻), it was of interest to examine the reaction between 1 and ethylene oxide (14); simple nucleophilic addition of CH₃O⁻ to 14 has been reported.⁴³ Although the reaction of 1 + 14 was very slow, the two major product-forming channels appeared to involve H⁻ and H⁺ abstraction processes by 1 (reactions 15a and 15b) producing anions *m/z* 65 (c-C₃H₅C⁻) and 43 (C₃H₅O⁻).⁴⁴

respectively. The ion m/z 43 is considered to be the enolate anion, $\text{H}_2\text{C}=\text{CHO}^-$.⁴⁴ Two minor product-forming channels (reactions 15c and 15d) yielded anions m/z 94 and 108.⁴⁴ The structure of the latter ion is reasonably assigned to that of the addition product, **15**. The ion m/z 94 may be $\text{C}_6\text{H}_6\text{O}^-$, formed by an



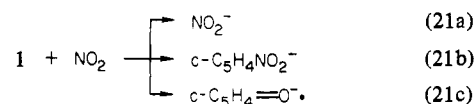
abnormal ring opening of **14** with **1**.

No reaction between **1** and nitrous oxide was observed. This result corroborates the conclusion reached from the protonation studies (above) concerning the electronic configuration of $\text{c-C}_5\text{H}_4^+$, $\sigma^1\pi^2$ vs. $\sigma^2\pi^1$. Considering that the $\sigma^2\pi^1$ electronic configuration of $\text{c-C}_5\text{H}_4^+$ is structurally related to that of the phenyl ($\text{c-C}_6\text{H}_5^+$) anion, reaction with N_2O would be expected to occur leading to anion products $\text{c-C}_5\text{H}_4\text{N}_2\text{O}^-$ (m/z 108) and $\text{c-C}_5\text{H}_4=\text{O}^-$ (m/z 80).²¹ The failure of **1** to react with N_2O is in keeping with the $\sigma^1\pi^2$ electronic configuration of **1** and the fact that $\text{c-C}_5\text{H}_5^-$ also fails to react with N_2O .

Bracketing the Ionization Potential of 1. The ionization potential (IP) of **1** is the electron affinity of the carbene cyclopentadienylidene ($c\text{-C}_5\text{H}_4$). MINDO/3 calculations of triplet ($\sigma^1\pi^1$) and singlet ($\sigma^0\pi^2$) $c\text{-C}_5\text{H}_4$ favor the triplet ($\Delta H_f^0 = 118.7$ kcal mol $^{-1}$) as the ground state by only 4 kcal mol $^{-1}$. This ordering is, at least, correct based on the ESR spectrum of the matrix isolated species.⁴⁵ The MINDO/3 geometries of **1** and triplet $c\text{-C}_5\text{H}_4$ are quite similar with the $\text{C}_5\text{-C}_1\text{-C}_2$ angles 114.4 and 117.8°, respectively; this angle in singlet $c\text{-C}_5\text{H}_4$ was 134.4°. This suggests that vertical ionization of **1** should yield triplet $c\text{-C}_5\text{H}_4$.

The rate of reaction of **1** with C_6F_6 was slow ($\sim 10^{-11} \text{ cm}^3 \text{ molecule}^{-1} \text{ s}^{-1}$) and the only product ion observed was m/z 231, the apparent result of aromatic substitution (reaction 22). No attempt was made to accurately determine the rate constant of reaction 22. This places a lower limit on $\text{IP}(\mathbf{1}) = \text{EA}(\text{C}_5\text{H}_4) \geq 41.5 \pm 7 \text{ kcal mol}^{-1}$.⁴⁶

With NO₂, the reaction with **1** was rapid (reaction 21, Table I) with three product-forming channels (reactions 21a-c). The



major product channel was charge transfer giving NO_2^- (m/z 46; m/z 47 ($M + 1$), obsd 1:0.004, theory 1:0.004; 47 ($M + 2$), obsd 1:0.004, theory 1:0.004). The second product channel yields what appears to be the product of radical-radical coupling, $\text{c-C}_3\text{H}_4\text{NO}_2^-$ (m/z 110; m/z 111 ($M + 1$), obsd. 1:0.065, theory 1:0.059).¹⁹ The minor, third product channel produced an anion m/z 80⁴⁴ which is probably the result of oxygen-atom transfer. The product distribution was found to be invariant with changes in the helium flow pressure (0.4–1.2 torr). The recent $\text{EA}(\text{NO}_2) = 54.4 \pm 2$ kcal mol⁻¹ from laser photodetachment of NO_2^- ^{47,48} establishes an upper limit to $\text{IP}(\text{I})$; therefore, 54.4 ± 2 kcal mol⁻¹ $\geq \text{IP}(\text{I}) = \text{EA}(\text{c-C}_3\text{H}_4) \geq 41.5 \pm 7$ kcal mol⁻¹. Laser photodetachment of a π electron from $\text{c-C}_3\text{H}_5^-$ giving $\text{c-C}_3\text{H}_5$ yields $\text{EA}(\text{c-C}_3\text{H}_5)$ ³⁴ = 41.2 ± 0.5 kcal mol⁻¹, which is within the above error limits of $\text{EA}(\text{c-C}_3\text{H}_4)$. This suggests that an electron is also lost from the π HOMO of **1** yielding triplet $\text{c-C}_3\text{H}_4$.

Summary and Conclusions

Structure of the Anion Radical $C_3H_4^-$. While it is reasonable to conclude that the structure of the anion radical m/z 64 produced by dissociative electron attachment to diazo compound **2** is c-

(43) Bierbaum, V. M.; DePuy, C. H.; Shapiro, R. H.; Stewart, J. H. *J. Am. Chem. Soc.* **1976**, *98*, 4229. No evidence for deprotonation of ethylene oxide by HO^- , H_2N^- , and CH_3O^- was observed.

(44) The product ion signal was too small to allow for accurate ($M + 1$) determinations. The molecular formula and structure of these ions must be considered as reasonable guesses at best.

(45) Wasserman, E.; Barash, L.; Trozzolo, A. M.; Murray, R. W.; Yager, W. A. *J. Am. Chem. Soc.* **1964**, *86*, 2304.

(46) Lifshitz, C.; Tiernan, T. O.; Hughes, B. M. *J. Chem. Phys.* **1973**, *59*, 3182.

(47) Herbst, E.; Patterson, T. A.; Lineberger, W. C. *J. Chem. Phys.* **1974**, *61*, 1300.

(48) For other values of $EA(NO_2)$ see: Janousek, B. K.; Brauman, J. I. In "Gas Phase Ion Chemistry", Bowers, M. T., Ed.; Academic Press: New York, 1979; Vol. 2.

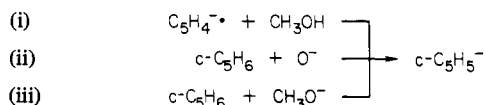
Table V. Thermochemical Data Evaluated in This Study at 298 K^a

		previous value ^a	ref
$\Delta H_f^\circ(1)$	$70.7 \pm 3.2,^b \geq 67.7 \pm 3^c$	$\leq 58 \pm 5$	18
PA(1)	377 ± 2		
EA(c-C ₅ H ₄)	$\leq 54.4 \pm 2, \geq 41.5 \pm 7$		
$D^\circ(\text{c-C}_5\text{H}_4\text{-H}^\cdot)$	$103.9 \pm 5.2,^b \geq 100.8 \pm 5^c$		

^a In kcal mol⁻¹. ^b From PA bracketing. ^c From H[·] affinity bracketing.

C₅H₄⁻, it was considered essential to establish beyond reasonable doubt the skeletal structure and electronic configuration of this anionic species. The following reactions of this species deal with these structural questions.

a. The same ion-molecule chemistry (rate constants and products) results from the anion product from the following three reactions;³² reactions ii¹⁸ and iii are known to yield c-C₅H₅⁻. These results confirm the skeletal structure of anion *m/z* 64 as c-C₅H₄⁻.



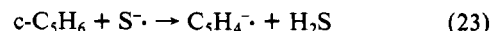
b. The radical behavior of anion *m/z* 64 is amply demonstrated by its H[·] abstraction reactions.

c. The reactivity of c-C₅H₄⁻ as a base toward proton donors, especially ROH, is in keeping with the structure of a π -delocalized anion, but not that of a σ -localized carbanion. This conclusion is supported by the failure of c-C₅H₄⁻ to react with N₂O.²¹

We, therefore, conclude that the anion radical *m/z* 64 produced from 2 in our FA experiments is c-C₅H₄⁻ with the $\sigma^1\pi^2$ electronic configuration as represented in 1.

Summary of Thermochemical Data from This Study. The important thermochemical data determined in the present study at 298 K are summarized in Table V.

The obvious disagreement in $\Delta H_f^\circ(1)$ determined in this study and that previously reported¹⁸ from the reaction



requires comment. Domenico et al.¹⁸ assumed that this reaction proceeded by α -elimination of H⁺ and H[·] from c-C₅H₆. We have been unable to produce anion *m/z* 64 by this reaction in the FA; the only observed product ion was c-C₅H₅⁻ (*m/z* 65). We calculate for eq 23 that $\Delta H_{rx} = +15.7 \pm 3.4$ kcal mol⁻¹.⁴⁹ We conclude that the elementary processes for eq 23 are not α -elimination of the geminal hydrogens from c-C₅H₆ by S[·].¹⁸ Further, using $\Delta H_f^\circ(1) \leq 58$ kcal mol⁻¹ yields an abnormally low value of $D^\circ(\text{c-C}_5\text{H}_4\text{-H}^\cdot) \leq 91.2 \pm 2$ kcal mol⁻¹.^{33,38}

The present results portray the power of the flowing afterglow method for determination of the intrinsic reactivities of reactive intermediates. The results of this approach have added another dimension to our understanding of the physical organic chemistry of hypovalent anion radicals in the absence of solution and ion-pair phenomena. Studies with other carbene anion radicals, and with various carbene cation radicals, are in progress.

Acknowledgment. We wish to express our sincere appreciation to Dr. John Kolts for the original design of our flowing afterglow and for discussions during its construction, and to Mr. Al Nielson for his talents and advice in the FA construction. We gratefully acknowledge support of this research from the U.S. Army Research Office (DAAG29-77-G-0142) and the National Science Foundation (Equipment Grant CHE76-80382).

(49) $\Delta H_f^\circ(\text{S}^\cdot) = 17.73$ kcal mol⁻¹.¹⁸ $\Delta H_f^\circ(\text{c-C}_5\text{H}_6) = 32.4$ kcal mol⁻¹.^{18,25} $\Delta H_f^\circ(\text{H}_2\text{S}) = -4.88 \pm 0.15$ kcal mol⁻¹.³¹

Oxidation of Amines by a 4a-Hydroperoxyflavin

Sheldon Ball and Thomas C. Bruice*

Contribution from the Department of Chemistry, University of California at Santa Barbara, Santa Barbara, California 93106. Received April 14, 1980

Abstract: Kinetic and product studies have been carried out for the reaction of 12 tertiary amines, secondary amines, and secondary hydroxylamines with the 4a-hydroperoxide of N⁵-ethyl-3-methylflavin (4a-FI₂OOH). All reactions were found to be first order in 4a-FI₂OOH and amine in *t*-BuOH solvent. Transfer from *t*-BuOH to the aprotic solvent dioxane decreases the second-order rate constant by ~threefold, but does not change the kinetic order in reactants (i.e., no external proton source is required). The reactions with the secondary and tertiary amines are quantitative, yielding secondary hydroxylamines and tertiary amine oxides along with the flavin pseudobase (4a-FI₂OH). Secondary hydroxylamines yield with 4a-FI₂OOH nitrones and 4a-FI₂OH. The free radical trap 2,6-di-*tert*-butyl-4-methylphenol does not influence the rate constants or product yields. This finding, along with the observation that rate constants are not related to the stability of cation radicals derived from amine, establishes that free radical processes are not involved in the N-oxidation reactions. The N-oxidation reactions are best explained as occurring through nucleophilic attack of amine nitrogen upon the terminal oxygen of the 4a-FI₂OOH molecule with back donation of the hydroperoxy hydrogen to the internal peroxy oxygen. Comparison of the second-order rate constants (on the basis of the amine pK_a's in H₂O) provides the nucleophilic order secondary hydroxylamines > tertiary amines > secondary amines. The disappearance of 4a-FI₂OOH from solution in the presence of primary amines is much slower than with secondary amines and the reaction does not follow a simple rate law nor is 4a-FI₂OH a major product. In *t*-BuOH the spontaneous first-order rate constant for decomposition of 4a-FI₂OOH exceeds that for the decomposition of H₂O₂ by more than 400-fold while the second-order rate constant for N-oxidation of *N,N*-dimethylbenzylamine by 4a-FI₂OOH exceeds that for N-oxidation by H₂O₂ by 36 000-fold (and N-oxidation by *t*-BuOOH by >400 000). These results are discussed in terms of the involvement of 4a-hydroperoxyflavin cofactor in the metabolism of amines by the hepatic flavoprotein microsomal oxidase.

Introduction

Mammalian liver contains two separate enzyme systems with different pathways for the oxidation of N-substituted amine drugs.¹ One system containing a flavoprotein (NADPH cytochrome P-450

reductase) and cytochrome P-450 catalyzes C-oxidation of amines resulting in N-dealkylation. The other system involves N-oxidation of secondary and tertiary amines catalyzed by a flavoprotein free of cytochromes, iron, and copper in an NADPH- and O₂-dependent process. Spectral studies establish that oxygen reacts with the reduced flavoprotein monooxygenase (Enz-FH₂) to form an enzyme-bound 4a-hydroperoxyflavin (Enz-4a-FI₂OOH).^{2,17} In

(1) B. S. S. Masters and D. M. Ziegler, *Arch. Biochem. Biophys.*, **145**, 358 (1971).